Ann. For. Res. 68(2): 97-116, 2025
https://doi.org/10.15287/afr.2025.4245

**ANNALS OF FOREST RESEARCH**
www.afrjournal.org

# Assessing spatial dynamics of GEDI biomass prediction in managed versus unmanaged tropical forest ecosystems in Kenya

**Erick O. Osewe[1], Mihai Daniel Niță[1], Mohamed Islam Keskes[1], Ibrahim Osewe[1], Ioan Vasile Abrudan[1]✉**

**Osewe E.O., Niță M.D., Keskes M.I., Osewe I., Abrudan I.V.,** 2025. Assessing spatial dynamics of GEDI biomass prediction in managed versus unmanaged tropical forest ecosystems in Kenya. Ann. For. Res. 68(2): 97-116.

**Abstract** Above ground biomass (AGB) estimation is vital for monitoring carbon storage and ecosystem fluxes, especially in tropical forests for climate mitigation in the Global South. The Global Ecosystem Dynamics Investigation (GEDI) instrument offers high resolution forest monitoring; however, field measurements are crucial to enhance spatial accuracy. This study assessed the limitations of using machine learning models trained on GEDI data to estimate AGB for two distinct forest ecosystems in Kenya: Kakamega National Forest Reserve (KNFR) and Karura Forest Reserve (KFR). Our specific objectives were (i) developing Random Forest (RF) machine learning model using GEDI data for training, (ii) comparing GEDI estimates with field measurements, and (iii) quantifying the limitations of using integrated GEDI-RF model. Plots were coincided with GEDI beams for comparison to assess variability and bias in AGB estimates. The p-value of 0.005 for heteroskedasticity in KNFR indicated high variability and bias of the GEDI-RF model relative to the field measured model. In contrast, p-value of 0.195 for heteroskedasticity in KFR indicated low variability and bias of the GEDI-RF model relative to the field measured model. 55% of plots which coincided with GEDI had less than 10% relative difference in AGB estimates between models. Plots outside of GEDI had a relative difference in AGB estimates between models greater than 10%. Relative to the field measured model, the GEDI-RF model overestimated AGB values less than 100 Mg $ha^{-1}$ and underestimated greater than 200 Mg $ha^{-1}$. This study contributes to effective forest monitoring, carbon accounting, and conservation in heterogeneous forests.

**Keywords:** GEDI, forest monitoring, remote sensing, tropical forest, carbon storage.

**Addresses:** [1]Faculty of Silviculture and Forest Engineering, Transilvania University of Brasov, Brasov, Romania.

✉ **Corresponding Author:** Ioan Vasile Abrudan (abrudan@unitbv.ro).

**Manuscript:** received July 7, 2025; revised July 31, 2025; accepted August 2, 2025.

## Introduction

Accurate predictions of Above Ground Biomass (AGB) in forests ecosystems are relevant for predicting terrestrial carbon changes (Feitosa et al. 2023) and implementing climate change mitigation programs, such as carbon trading schemes (Chirici et al. 2022). For instance, climate mitigation programs like reducing emissions from deforestation and forest degradation (REDD+) in the Congo basin and Amazon rainforest heavily relies on credibility and accuracy of AGB predictions (Demarchi et al. 2023, Morgan et al. 2023). Similarly, the European Union (EU) transition towards renewable energy in some member states highlights forest biomass as a necessary precursor to a successful bioeconomy (Kikuchi et al. 2018). Therefore, AGB estimations allow optimization of forest resources and improve our understanding of vital forest functions (Augusto & Boča 2022).

Assessments providing AGB estimations facilitate the evaluation of ecosystem services (ES) and ecological monitoring, which are vital for determining the state of forest ecosystems with reference to biodiversity and productivity on a spatial-temporal scale (Schneider et al. 2021).

Approaches in AGB estimation have favoured remote sensing methods because they offer relative accuracy in prediction in the context of spatial-temporal dynamics for large and inaccessible forest ecosystems (Rodrigues et al. 2023, Ma et al. 2024). Within the tropics, traditional methods for biomass estimation that utilize allometric equations (Adinugroho et al. 2023), which typically involve individual tree measurements of tree diameter at breast height (DBH), wood density (WD) and tree height (H), are expensive especially for those requiring periodic monitoring in forest research. Sebrala et al. (2022a) similarly identified the high costs of data acquisition at plot level as a key limiting factor in forest monitoring within the Global South.

Research highlighting changes in carbon levels through the monitoring of forest biomass are more comprehensive in the Global North as opposed to the Global South (Tetere & Zeverte-Rivza 2023, Munteanu et al. 2024).

In the Global South, where tropical forests play a critical role in climate mitigation (Nesha et al. 2021), few countries have established National Forest Inventories (NFI). The NFI consist of temporary and permanent plots established in different forest ecosystems to assist in the long-term monitoring and systematic assessments of forest stock at national level (Tomppo 2004).

While remote sensing approaches have several advantages with evolving technologies to reduce uncertainty of AGB predictions, many studies have highlighted the variations in spatial, spectral reflectance, and temporal resolutions (Osewe et al. 2022), which affect quality of optical data for processing (Dutca et al. 2019, Osewe & Dutca 2021).

Complex stand structures and species variability found in dense tropical rainforest ecosystems contribute to the uncertainties associated with prediction of AGB (Moundounga Mavouroulou et al. 2014).

Approaches that heavily rely on remote sensed data without plot data validation have yet to fully capture the critical ecological functions essential for maintenance of global biodiversity (Hemingway & Opalach 2024), and climate regulation (Francini et al. 2023).

Integration approaches seeking to avert collinearity using allometric biomass models and remote sensed radar data are also influenced by signal saturation (Joshi et al. 2017), which limit their ability for accurate predictions (Hansen et al. 2013).

High acquisition costs associated with airborne lidar technologies (Shannon et al. 2022), and field surveys methods which provide detailed measurements of tree biometrics and stand structure with relatively lower standard of error, prohibit their widescale application within the Global South (Ramachandran et al. 2023).

To address the gap of improving forest canopy observations by providing comprehensive details on forest and vegetative structure, the Global Ecosystem Dynamics Investigation

(GEDI) instrument offers a practical and convenient alternative (Silva et al. 2021).

GEDI is a spaceborne high-resolution lidar instrument on the international space station (ISS) that uses pulses of laser light to measure three-dimensional structures on the earth's surface (Dubayah et al. 2020). From GEDI, the observable waveforms provide information on canopy height, vertical structure, topography, and canopy cover (Bruening et al. 2023, Magruder et al. 2024).

The expansive coverage of GEDI between 51.6° N to 51.6° S over tropical and temperate forest avails the much-needed information on canopy height, canopy cover and tree vertical profiles which could be integrated with data from high-resolution satellites like Landsat and MODIS to carry out modelling of dense forest ecosystems (Narin et al. 2024).

The detailed analysis of forest structure infers information about suitability of habitats, which is an indicator for biodiversity and species distribution (Osewe et al. 2022, Brodie et al. 2023).

In the comparative analysis between spaceborne lidar instruments of GEDI and the Ice, Cloud, and Land Elevation Satellite-2 (ICESat-2), Urbazaev et al. (2022) concluded that both instruments exhibited a high level of accuracy for estimation of terrain elevation measurements in most of the major forest types except for tropical upland forests, where GEDI performed relatively better owing to the signal threshold (Hancock et al. 2019a).

Furthermore, Mohite et al. (2024) established that data fusions which incorporate species- and site-specific forest aspects in India improved predictor accuracy of GEDI when integrated with other satellite data sources for AGB estimation. In Spain, Quiros et al. (2021) highlighted efficiency of combined model approaches to avert limitations of point sampling resolution grids from the GEDI. Similar studies (Gelabert et al. 2024, Stan et al. 2024) have also suggested integration of ground validation data to improve the accuracy of AGB estimations using GEDI.

Previous studies (Murrins Misiukas et al. 2021, Fassnacht et al. 2024), using remote sensing approaches to estimate AGB for tropical forest ecosystems, have highlighted the limitations associated with the lack of plot level measurements which could provide the local context, existing ecological variations, and data for validation.

This research addresses the gap by incorporating individual tree measurements i.e., DBH, H, and species obtained at plot level using the Arboreal-digital calliper (Lindberg 2020) to compare with measurements from GEDI. The Arboreal digital calliper is an alternative to traditional methods of field data collection in forest research which are typically laborious, expert dependent and expensive. Other studies have also concluded that Arboreal-digital calliper is an accurate alternative in the assessment of three similar applications i.e., Trestima app, Katam app and Arboreal (Sandim et al. 2023).

Our approach leverages on GEDI to provide high quality details on the canopy cover and vertical structures (Pascual et al. 2023) for two different forest ecosystem types (tropical unmanaged rainforest versus urban managed forest) and to reference them with sample plot data that are positioned along a line transect to coincide with GEDI sensor beams for accurate comparison.

This study builds on ongoing research seeking to improve methodologies for AGB estimations using GEDI for tropical regions in the Global South that lack NFI data (Calders et al. 2023, Wang et al. 2024a). This study assessed the limitations of using machine learning models trained on GEDI data to estimate AGB for two distinct forest ecosystems in Kenya: Kakamega National Forest Reserve (KNFR) and Karura Forest Reserve (KFR).

Our specific objectives were (i) to develop Random Forest (RF) machine-learning model using GEDI data for training, (ii) to compare GEDI estimates with field measurements, and (iii) to quantify the limitations of using integrated GEDI-RF model.

## Materials and Methods

### Study area

Our study areas consist of two different forest ecosystems in Kenya detailed in Figure 1, KNFR with a current size of 19,792.4 ha, which is the last remaining intact tropical rainforest in Kenya (Bleher et al. 2006, Osewe et al. 2022) and KFR with the size of 1,041 ha, which is an important urban forest ecosystem in the capital city of Nairobi (Manji 2017).

This comparative assessment of two different forest ecosystems provides insights into the impact of forest type variations on AGB estimates i.e., the effect of species composition and diversity (Yao et al. 2022), the effect of forest structure and stand density (Ullah et al. 2021), the effect of tree age and succession stages (Rozendaal et al. 2022) and the impact of disturbance and management regimes on AGB estimation (Shi et al. 2021).

The sampling regime for KNFR accommodated the heterogeneity of species amongst the three national reserves (Kakamega Forest Reserve, Kakamega National Reserve and Kisere National Reserve) and two nature reserves (Isecheno and Yala) (Osewe et al. 2022). In KFR, the plot sampling accommodated the heterogeneity of species by capturing the silvicultural treatments i.e., undisturbed indigenous sections, planted sections which were cleared and replanted under various regimes and undisturbed old-growth forest sections (Keige 2019).

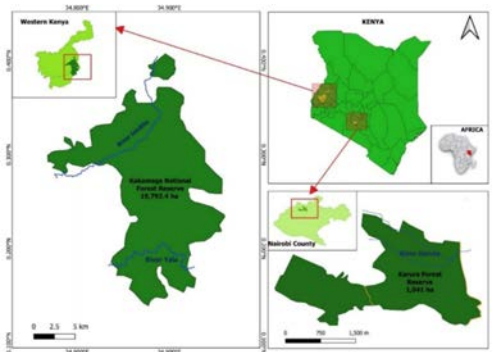


**Figure 1** Map of study areas in Kenya.

### Data

This study leveraged on data from GEDI by creating a region of interests (ROI) with coordinates to provide relevant information on canopy cover, height, and vertical tree profile metrics for KNFR and KFR. The data products based on the ROI were accessed from GEDI Level 2B canopy cover and vertical profile metrics product (Dubayah 2021). To obtain high quality data, only GEDI waveforms with fidelity greater than 0.95 were selected (Zhang et al. 2022), which had footprints transecting respective study areas.

The dataset was further filtered by applying a maximum allowable difference of 50 meters between the lowest elevation detected by GEDI and the actual terrain elevation (Pascual et al. 2025).

The downloaded data from GEDI Level 2B product in hierarchical data format was converted to a spatial points data frame using a customised R-script based on Silva et al. (2018) in R-studio software.

The spatial points data frame variables were exported as shapefiles compatible with open-source geographic information system software (QGIS).

Using QGIS software (QGIS Project, 2023), the shapefiles were analysed to provide visual representation of the forest canopy cover, vertical structure, precise references for latitude and longitude along the path of GEDI laser beams of 25 meters footprint (Hancock et al. 2019b).

Coordinates of sample plots in both KNFR and KFR were determined based on the precise latitude and longitude references to coincide with the path of GEDI laser beam on QGIS software as shown in Figure 2.

Plot sampling regime were established to accommodate the heterogeneity of species, disturbance and stand development stages i.e., stand initiation stage to old growth stages for KNFR and KFR.

To capture ecosystem variability of the two different forest types, sample plots were evenly distributed at consecutive 60 m intervals coinciding with the GEDI path in a line transect format progressing inwards from the forest edge as detailed Figure 2.

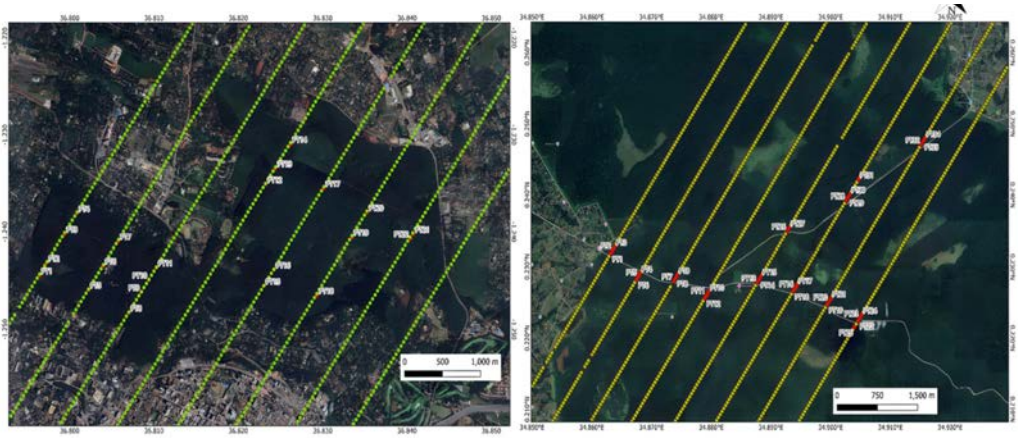

(a) Excerpt of plots (PT) aligned with GEDI laser beam path in Karura Forest Reserve

(b) Excerpt of plots (PT) aligned with GEDI laser beam path in Kakamega National Forest Reserve

**Figure 2** Excerpt of plot sampling regime aligned with GEDI laser beam path.

We overlaid required specifications on a lidar-enabled handheld device to establish circular plots of size 500 $m^2$, with the centre determined using coinciding coordinates and the boundary extent on a real-world environment through an augmented reality (AR) platform (Tom Dieck et al. 2021) created by the Arboreal application (Lindberg 2020).

With the generated perceptual information, we identified individual trees as shown in Figure 3 within each plot and measured their diameters ≥ 10 cm at 1.3 meters (DBH).

The Arboreal application offers high accuracy with negligible difference compared to traditional methods of using calliper or tape. For instance, Borz et al. (2024) statistically compared accuracy in measurement of DBH using Arboreal application with callipers in forest survey and determined a high degree of concurrence. Sandim et al. (2023) similarly highlighted reliability of the Arboreal application towards averting limitations of cost in data acquisition and time spent in the field plots during measurements.

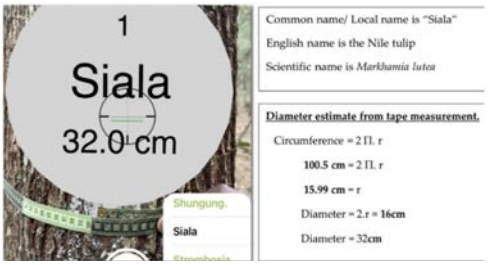


**Figure 3** Field measurement of DBH using Arboreal digital calliper.

Within the AR environment, measured trees were virtually tagged to avoid duplication in measurement, to show species and the fixed positions of trees within each plot. Arboreal application estimated the average H measurement per species within every plot based on the DBH measured. In KFR and KNFR, we identified a total of 47 unique tree species and measured the DBH for a total of 1445 trees in KNFR (34 plots) and 1603 trees in KFR (32 plots). A minimum of three plots per GEDI path were selected based on footprint distribution across major forest types in KNFR and KFR, ensuring representativeness of the ecosystem.

## Data Processing

### *Estimating AGB using a machine-learning model with GEDI data as training*

The data was processed using a series of steps: indices were first extracted from Sentinel-2 satellite imagery and elevation data from the Shuttle Radar Topography Mission (SRTM). These indices were used to extract predictors for developing a machine-learning model. The model was trained using GEDI data.

### *Image and auxiliary data processing*

To process the data, images within the ROI with less than 5% cloudy pixels were filtered, creating a median composite. This composite was reprojected to the specified projection system (EPSG: 4326) and rescaled to a 10-meter pixel size (Wen et al. 2024). We also incorporated the dataset from the SRTM mission version 4 to provide accurate elevation information and high-resolution information about the terrain, allowing for detailed measurements of elevation within the study areas. Moreover, the SRTM dataset enhanced our understanding of the topographical features and characteristics in the study area's terrain (NASA Jet Propulsion Laboratory 2024).

### *Predictors extraction*

Predictors emerged as a refined dataset after applying filtering and processing techniques to a range of band combinations and indices from Sentinel-2 satellite images. These images were only used in the extraction of predictors for developing the machine-learning model. They included the NDVI (Normalized Difference Vegetation Index) which facilitated the identification of vegetated areas by contrasting near-infrared and red-light reflectance (Basak et al. 2023), the Shadow Index (SI) excels that detected shadows, and the SAVI (Soil-Adjusted Vegetation Index) which assessed vegetation by adjusting for soil brightness (Fadl et al. 2024).

The EVI (Enhanced Vegetation Index) improved sensitivity in challenging environmental conditions, whereas the BI (Bare Soil Index) highlighted areas devoid of vegetation, such as bare soil or mineral surfaces (Wang et al. 2024b).

Finally, the NDII (Normalized Difference Infrared Index) evaluated plant moisture levels through infrared light analysis (Alados et al. 2022). These indices augmented the band information and enhanced the analysis of vegetation and shadow characteristics, expanding the analytical capabilities of the image processing approach (Boali et al. 2024).

### *Machine-learning modelling*

A machine-learning algorithm model was developed using GEDI data as input (Vrtač et al. 2024). Specifically, we used the RF algorithm (Khajavi & Rastgoo 2023). Breiman (2001) highlighted the effectiveness of RF as an algorithm in supervised learning to minimize prediction variance by combining multiple decision to generate random subsets of data (Zhang et al. 2024). Each tree in the forest was trained on a random subset of the training data and features. At test time, the random forest took the average (for regression) or majority vote (for classification) of the predictions from each of the individual trees to make its final prediction (Cha et al. 2021).

The hyperparameters of the RF algorithm, including critical parameters, such as the number of trees, maximum depth, minimum samples per split, and the number of features considered for splitting at each node, were meticulously optimized using a grid search approach (Bischl et al. 2023). This method systematically evaluated the model's performance by exhaustively testing all possible combinations of hyperparameter values within a predefined range (Niu et al. 2020). This approach ensured the selection of the configuration that not only maximized predictive accuracy, but also minimized overfitting (Probst et al. 2019), enabling the model to generalize effectively unseen data.

Previous studies have stated the effectiveness of the RF algorithm when dealing with intricate and nonlinear decision boundaries, making it suitable for both categorical and continuous target variables (Nieto et al. 2024, Sarkar et al. 2024). It has also proven capabilities in managing datasets with noise and high dimensionality (Divasón et al. 2023), showcasing resilience against overfitting and enhancing the overall generalization performance of the model (Ramampiandra et al. 2023, Vuillod et al. 2024).

The RF incorporates randomization techniques in feature selection and training data for each tree, minimizing the correlation among trees (Sun et al. 2024), and enhancing model accuracy (Lei et al. 2024). Therefore, RF performs well when handling large datasets characterized by numerous variables and intricate interactions (Mellor et al. 2015), which makes it suitable for our two study areas (Lee et al. 2024).

To check our model performance relative to the field measured AGB estimates, we tested heteroskedasticity to assess bias using the Bland-Altman analysis (Giavarina 2015).

### *Estimating AGB based on field measurements*

To estimate AGB based on the field measurements, we used non-destructive approaches (Krause et al. 2023) by exploring available literature for species-specific allometric equations (Appendix, Table AI) for the most abundant species.

For the less occurring species, we used site-specific allometric equations (Kuyah et al. 2012, Nyamukuru et al. 2023), and used the same allometric equations for trees with similar growth rates when species-specific equations were unavailable (Sebrala et al. 2022b). Similar studies have established that species and site-specific allometric equations reduce levels of uncertainty associated with ecotype variations in AGB estimation (Pati et al. 2022, Mulatu et al. 2024).

All the allometric equations incorporated in the R-studio script relied on DBH as the only variable with specie-specific coefficients to account for the uncertainty (Picard et al. 2012). Within the R-studio, we defined functions based on the allometric equations to calculate the biomass for each species.

The results were compiled into a list corresponding to each of the tree species. The AGB estimate for each tree species was added as a new column to the dataset, and a total estimate was calculated for each plot in the study areas.

Using the Shapiro-Wilk Test in R Studio (Das & Imon 2016), we checked the normality of the distribution of the differences between the AGB estimate from field measurements and the AGB estimate from the integrated GEDI-RF to determine the appropriate statistical test. For a normal distribution of data, a paired t-test is appropriate (Krzywinski et al. 2014). For data not normally distributed, a Wilcoxon Signed-Rank Test is appropriate (Rey & Neuhäuser 2011).

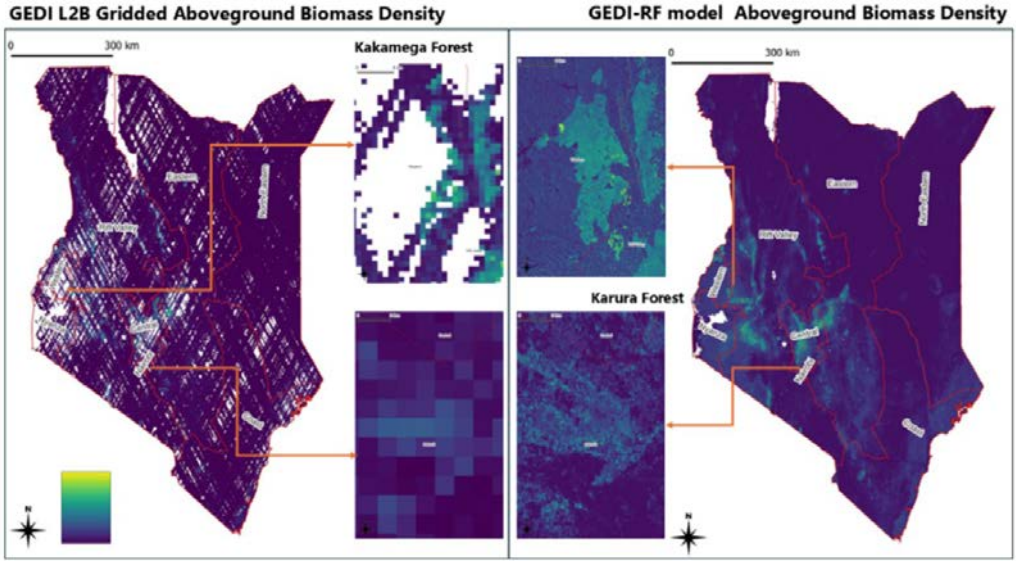


**Figure 4** Estimating AGB with wall-to-wall coverage from integrated GEDI-RF model.

## Results

### Estimating the AGB using GEDI with the RF machine-learning model

The GEDI beams provided extensive coverage of the country, with available footprints of spatial resolution 25 metres in a gridded format resulting in gaps in certain areas as shown in Figure 4.

The aggregation of data to a 1 km resolution in GEDI product smoothed out spatial variability and missed finer scale landscape features because of the 600 m spacing footprints across track. This meant that some areas within each 1 km lacked direct GEDI measurements. This was averted by integrating the RF machine-learning model trained on GEDI data to generate continuous wall-to-wall AGB estimates at 10 m resolution, effectively filling in the gap within gridded areas where GEDI footprint was absent to provide a complete spatial coverage in all areas.

At a 10-meter resolution, the integrated GEDI-RF model captured finer details within the study areas by filling the gaps from GEDI data to produce continuous AGB estimation. Based on the integrated GEDI-RF model, the total AGB estimate for the county was 2.36 billion Mg, which is equivalent to 1,108 Mt $CO_2e$ according to the Intergovernmental Panel on Climate Change (IPCC) conversion factor (Clarke & Wei 2023).

### Regional AGB estimates in Kenya

At regional level, there were high estimates of AGB between 117.4 to 245.4 Mg ha$^{-1}$ and 94.3 to 117.4 Mg ha$^{-1}$ in the Western, Southwestern and Central regions of Kenya as detailed in Figure 5. Moderate

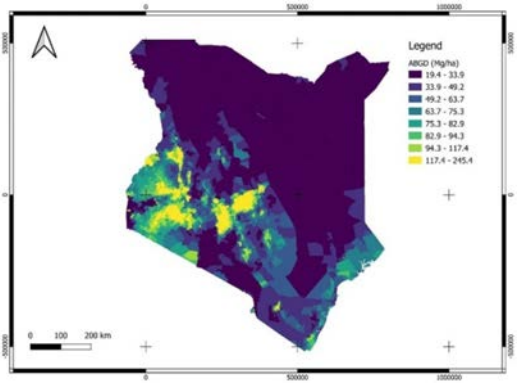


**Figure 5** AGB estimates for the different regions in Kenya.

estimates of AGB ranging from 63.7 to 82.9 Mg ha$^{-1}$ were in the Central region, while moderate to high estimates ranging from 49.2 to 94.3 Mg ha$^{-1}$ were in the Southeastern region. Low AGB estimates ranging from 19.4 to 33.9 Mg ha$^{-1}$ were noticeable to Northern and Northeastern Kenya.

### Estimates for KFR (managed urban forest) versus KNFR (unmanaged rainforest)

AGB estimates for the study areas of KFR and KNFR were extracted and summarised in Table 1. KNFR, which is in the Western region of the county, had higher AGB and AGB density compared to KFR, found in the Central region. The standard deviation (SD) for both areas represented variability in AGB estimates, where KNFR had a greater range in AGB values compared to KFR.

### Comparing integrated GEDI-RF model with field-measured AGB estimates

Out of the total 65 plots across both study areas, 40 coincided with the GEDI path (Table 2), while 25 were outside of the GEDI path (Table 3).

**Table 1** AGB estimates for the study areas in Kenya.

| Study area | Sum of AGB (Mg) | AGBD (Mg ha$^{-1}$) | (SD) | Carbon ($CO_2e$) | Monetary value of Carbon |
|---|---|---|---|---|---|
| KNFR | 4,381,877 | 177 | 62 | 2,059,482 | 123,568,920 |
| KFR | 114,307 | 106 | 36 | 53,724 | 3,223,440 |
| Total net values for study areas | | | | ∑ 2,113,206 | ∑ 126,792,360 |

Carbon ($CO_2e$): Carbon ($CO_2e$) equivalent in metric /tons IPCC conversion factor (Clarke & Wei 2023), AGB x 0.47 Carbon = ($CO_2e$); Monetary value of Carbon: Estimated monetary value of Carbon in US$ per metric ton of ($CO_2e$) according to the EU Emission Trading Scheme (EU, 2024).

**Table 2** Comparing AGB estimates from GEDI-RF model with field data for coinciding plots.

| Study areas | Field Plots GEDI path | AGB field eq. (Mg ha$^{-1}$) | AGB GEDI-RF model (Mg ha$^{-1}$) | Relative difference (%) |
|---|---|---|---|---|
| (0) | Unique plot codes (1) | Field AGB (2) | *GEDI - RF AGB* (3) | 100*[(2)-(3)]/(2) |
| KNFR | 81347 | 98 | 101 | 3.06 |
| | 81348 | 188 | 200 | 6.38 |
| | 81349 | 234 | 238 | 1.71 |
| | 81353 | 299 | 349 | 16.72 |
| | 81356 | 379 | 390 | 2.9 |
| | 81392 | 169 | 179 | 5.92 |
| | 81393 | 205 | 237 | 15.61 |
| | 81589 | 343 | 396 | 15.45 |
| | 81590 | 325 | 347 | 6.77 |
| | 81592 | 174 | 206 | 18.39 |
| | 81593 | 268 | 310 | 15.67 |
| | 81595 | 183 | 208 | 13.66 |
| | 81596 | 361 | 409 | 13.3 |
| | 81666 | 283 | 330 | 16.61 |
| | 81667 | 263 | 304 | 15.59 |
| | 81668 | 281 | 312 | 11.03 |
| | 81670 | 177 | 189 | 6.78 |
| | 81887 | 356 | 368 | 3.37 |
| | 81888 | 225 | 259 | 15.11 |
| | 81890 | 236 | 273 | 15.68 |
| | 81892 | 188 | 206 | 9.57 |
| | 81893 | 93 | 103 | 10.75 |
| | 81895 | 272 | 287 | 5.51 |
| KFR | 72817 | 92 | 100 | 8.7 |
| | 72823 | 185 | 204 | 10.27 |
| | 74115 | 39 | 40 | 2.56 |
| | 74133 | 68 | 80 | 17.65 |
| | 74262 | 213 | 220 | 3.29 |
| | 74298 | 143 | 168 | 17.48 |
| | 74308 | 112 | 121 | 8.04 |
| | 74544 | 123 | 133 | 8.13 |
| | 74577 | 106 | 113 | 6.6 |
| | 74635 | 71 | 72 | 1.41 |
| | 74636 | 112 | 124 | 10.71 |
| | 74642 | 138 | 144 | 4.35 |
| | 75130 | 290 | 307 | 5.86 |
| | 75137 | 101 | 115 | 13.86 |
| | 75164 | 58 | 59 | 1.72 |
| | 75183 | 125 | 133 | 6.4 |
| | 75543 | 272 | 287 | 5.51 |

Field Plots GEDI path: Field Plots coinciding with GEDI path; AGB field eq.: AGB estimate from field measurements with allometric equations (Appendix, Table AI); AGB GEDI-

RF model: AGB estimate from integrated GEDI-RF model; Relative Difference: Relative difference between models in AGB estimation (%) (values are presented as absolute percentages).

**Table 3** Comparing AGB estimates from GEDI-RF model with field data outside of GEDI path.

| Study areas | Field Plots GEDI path | AGB field eq. (Mg ha$^{-1}$) | AGB GEDI-RF model (Mg ha$^{-1}$) | Relative difference (%) |
|---|---|---|---|---|
| (0) | Unique plot codes (1) | Field AGB (2) | *GEDI - RF AGB* (3) | 100*[(2)-(3)]/(2) |
| KNFR | 81355 | 313 | 393 | 25.56 |
| | 81391 | 142 | 174 | 22.54 |
| | 81588 | 374 | 454 | 21.39 |
| | 81591 | 188 | 253 | 34.57 |
| | 81600 | 81 | 105 | 29.63 |
| | 81669 | 244 | 318 | 30.33 |
| | 81671 | 171 | 218 | 27.49 |
| | 81672 | 227 | 291 | 28.19 |
| | 81889 | 71 | 96 | 35.21 |
| | 81891 | 132 | 175 | 32.58 |
| | 81894 | 80 | 97 | 21.25 |
| KFR | 73520 | 98 | 124 | 26.53 |
| | 74084 | 121 | 183 | 51.24 |
| | 74092 | 54 | 79 | 46.3 |
| | 74161 | 82 | 102 | 24.39 |
| | 74294 | 44 | 55 | 25 |
| | 74295 | 147 | 197 | 34.01 |
| | 74309 | 49 | 70 | 42.86 |
| | 74520 | 165 | 197 | 19.39 |
| | 74567 | 54 | 65 | 20.37 |
| | 74604 | 44 | 58 | 31.82 |
| | 74654 | 126 | 163 | 29.37 |
| | 74660 | 68 | 110 | 61.76 |
| | 74661 | 45 | 59 | 31.11 |
| | 75536 | 62 | 79 | 27.42 |
| | 75550 | 21 | 27 | 28.57 |

Field Plots GEDI path: Field Plots coinciding with GEDI path; AGB field eq.: AGB estimate from field measurements with allometric equations (Appendix, Table AI); AGB GEDI-RF model: AGB estimate from integrated GEDI-RF model; Relative Difference: Relative difference between models in AGB estimation (%) (values are presented as absolute percentages).

AGB estimates from field measurements with allometric equations were compared in both cases to assess the relative differences between the two estimation models. The relative differences between AGB estimates from the field measurements of plots coinciding with the GEDI path compared to the integrated GEDI-RF model had low to moderate variability, ranging from 1.41% to 18.39% relative difference across both study areas. The two models showed alignment in AGB estimates in both study areas where 55% of plots which coincided with the GEDI path had a relative difference of ≤ 10% between models.

The relative differences between the AGB estimates from field measurements outside of the GEDI path compared with the integrated GEDI-RF model had high variability, ranging from 19.39% to 61.76% across both study areas in Table 3. Compared to the findings in Table 2, the plots outside of the GEDI path in both study areas had relative differences with all values falling ≥ 10%, indicating discrepancies in the AGB estimation associated with non-alignment with the GEDI.

In both scenarios of plotting, the Shapiro-Wilk test p-value of 0.025 indicated that the differences between field measurements and GEDI-RF estimates were not normally distributed. Furthermore, the Wilcoxon Signed-Rank Test p-value less than 0.001 indicated that the GEDI-RF model had higher estimates of AGB compared to field-measured estimates in both plot scenarios.

## Relative difference in AGB estimates under two scenarios of plot measured data

The median relative difference at 9.57% was smaller for plots coinciding with the GEDI path compared to plots outside the GEDI path at 29.37% as shown in Figure 6. The AGB estimates from both models aligned when field plots coincided with the GEDI path. The interquartile range was smaller for plots coinciding with the GEDI path at 7% compared to plots outside at 11%, indicating less variability. Further, Figure 6 (a) had fewer outliers and shorter whisker length compared to Figure 6 (b) which meant that the integrated GEDI-RF model was consistent in estimating AGB for plots coinciding with the GEDI path compared to those outside the path.

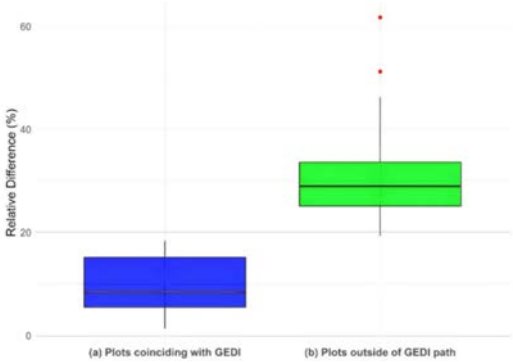


**Figure 6** Comparing relative differences in AGB estimates under two scenarios of plot data.

## Observed limitations in the AGB estimation

This study identified four major limitations: exclusion of individual tree height as a variable in the field-measured allometric model, field measurements restricted to DBH ≥ 10 cm, substitution of species-specific and site-specific allometric equations, and the limitation of GEDI-RF model relative to the field-measured allometric model.

## Exclusion of individual tree height variable in the field-measured allometric model

Individual tree height variable from trees within plots was not captured by the Arboreal digital calliper, rather an average of height measurement per species within the plots was captured. Therefore, only individually measured tree diameters ≥ 10 cm at 1.3 meters (DBH) were used as a single parameter in the allometric equations for AGB estimation (Appendix, Table AI). DBH is a strong predictor of AGB, 55% of the plots that coincided with the GEDI path displayed a relative difference in AGB estimates between models of ≤ 10%. Plots outside of the GEDI path and had a relative difference in AGB estimates between models from 19.39% to 61.76% with many outliers as detailed in Figure 6.

### *Field measurement of tree DBH ≥ 10cm*

Only trees with DBH ≥ 10 cm were measured per plot, excluding small trees of ≤ 10 cm in DBH, which also collectively contribute to the overall AGB. The GEDI-RF model in Figure 4 captured finer details within the study areas to produce continuous AGB estimation, which contrasts with the underestimation of AGB from the field-measured model in Table 2 and Table 3. Although this threshold is a practical consideration of field-measurement time and effort, the p-value less than 0.001 from the Wilcoxon Signed-Rank Test indicated that the GEDI-RF model had higher estimates of AGB compared to field-measured estimates. Therefore, it results a bias towards younger forests and regenerating stands which were captured by the GEDI RF model as detailed in Figure 7.

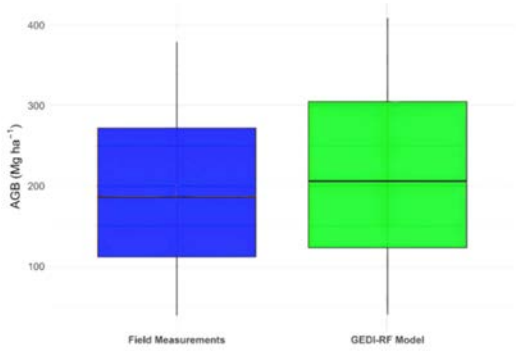


**Figure 7** Comparing AGB estimates from field measurements versus GEDI-RF model.

## Limitations of the GEDI-RF model relative to the field-measured AGB estimates

The Bland-Altman plot demonstrates the systematic tendency of the GEDI-RF model performance depending on the range of AGB values based on the levels of agreement between mean AGB estimates from the field-measured model and the GEDI-RF model. In both KNFR and KFR, the GEDI-RF model relative to the field-measured model had overestimated AGB values ≤ 100 Mg ha$^{-1}$ and underestimated ≥ 200 Mg ha$^{-1}$ as shown in Figure 8.

The p-value of 0.005 was statistically significant for heteroskedasticity in KNFR, which indicated high variability and bias of the GEDI-RF model relative to the field-measured model across the range of AGB values. In contrast, the p-value of 0.195 was not statistically significant for heteroskedasticity in KFR, which indicates low variability and bias of the GEDI-RF model relative to the field-measured model across the AGB values.

## Substitution of species-specific and site-specific allometric equations in biomass prediction

For the identified species in both KNFR and KFR, we used species-specific allometric equations in estimating the AGB from field measurements (Appendix, Table AI). In KNFR, the species endemic to this ecosystem lacked tested allometric equations. The p-value of 0.005 for heteroskedasticity in KNFR indicated high variability and bias of the GEDI-RF model relative to the field-measured model. While this approach allowed us to estimate the AGB, it entailed biases in estimation, particularly for endemic species with unique traits not captured by the substituted equations.

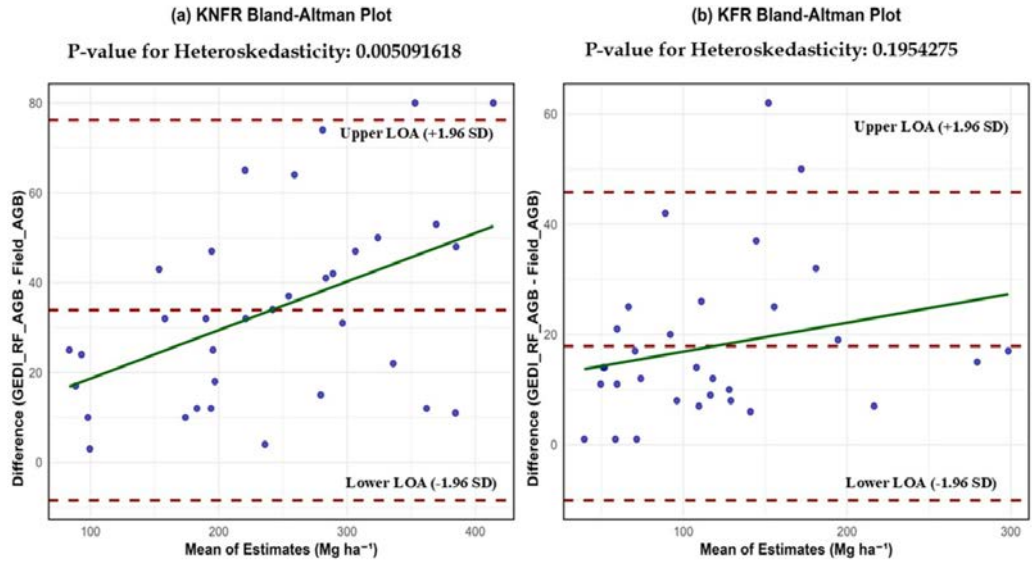


**Figure 8** Heteroskedasticity test between the GEDI-RF model and field-measured model.

## Discussion

The differences of forest stand structure in managed (KFR) compared to unmanaged (KNFR) forest ecosystems influenced GEDI waveform penetration and affected AGB estimates (Navarro et al. 2019, Ullah et al. 2021). The GEDI-RF model relative to the field measurements from 34 plots had a p-value of 0.005 for heteroskedasticity which exhibited high variability and low precision in AGB estimates in KNFR, an unmanaged tropical rainforest ecosystem (Fayad et al. 2022).

For KFR, a managed urban forest ecosystem with silvicultural treatments, GEDI-RF model relative to the field measurements from 32 plots had a p-value of 0.195 for heteroskedasticity which demonstrated low variability and high precision (Hakkenberg et al. 2023). Tian et al. (2023) similarly found that factors like the error propagation, stand structure and the uncertainty of remote sensing greatly impact the AGB estimation.

Other studies have also integrated GEDI with multispectral synthetic aperture radar (SAR) (Nandy et al. 2021, Liu et al. 2024) to produce an end-to-end spatially continuous resolution of study sites.

RF machine learning models have also been used to improve performance and avert negative variability in AGB estimates (Zhu et al. 2020).

Our study provided insight on biomass prediction variability by leveraging on field-measured estimates from managed (KFR) and unmanaged (KNFR) forest ecosystems to assess bias and variability in AGB estimation when using the GEDI-RF model. 55% of field-measured estimates which coincided with GEDI path had ≤ 10% relative difference in AGB estimates between GEDI-RF model relative to the field data-based model. Therefore, improvements in full spectral coverage and AGB estimation in both study areas occurred because of the integrated GEDI-RF model.

Tropical rainforests classified as old-growth forest with dense structure and mature stands, characteristically made up of tall, closed canopies obscure the understory and affect waveform penetration for satellite instruments estimating AGB (Fagua et al. 2021, Gonçalves et al. 2017). These factors contributed to the high variability and bias of the GEDI-RF model relative to the field-measured model (Baban & Niţă 2023). Moreover, KNFR maintains a dense closed canopy resulting from its protected status and the absence of silvicultural management practices (Republic of Kenya, 2016).

However, it also faces threats from land use changes, such as agricultural expansion along the forest edge (Osewe et al. 2022). Hunka et al. (2024) similarly find that GEDI has high variance in AGB estimation for closed canopy old growth forest which contributes towards high levels of uncertainty. In contrast, we find that in KFR, the GEDI-RF model estimates were comparable relative to field-measured estimates with negligible differences in accuracy. This is because KFR mainly comprises pure stands and mixed stands in a managed secondary forest set up (≤ 20 years), that did not present waveform hindrances (Pretzsch et al. 2017).

Further, other studies using remote sensing hyperspectral instruments also reported effective capture of stand structures for urban forest ecosystems without waveform obstruction (Ferreira et al. 2024). The p-value less than 0.001 from the Wilcoxon Signed-Rank Test indicated that the GEDI-RF model had higher estimates of AGB relative to field measured estimates across both study areas owing to the full capture of all stands (young stands and regeneration strands), with few hindrances in dense multilayered canopies (Dorado-Roda et al. 2021, Potapov et al. 2021).

The GEDI-RF model improved the accuracy of AGB estimates by filling the gaps in areas where gridded GEDI footprints were absent (Kellner et al. 2023). At a national level, the GEDI-RF model generated continuous wall-to-wall AGB estimates at a 10-meter resolution and captured finer details to estimate AGB with comparable accuracy (Jia et al. 2024, Li et al. 2024). Similar approaches have integrated GEDI with machine learning models to improve prediction accuracy (Singha & Sahoo 2024).

We find high AGB density estimates in the Western, Southwestern and Central regions of Kenya. These regions are predominantly montane forests, like the Mau Forest complex (Tarus & Nadir 2020), and western tropical rainforest, such as Nandi North, Nandi South and KNFR (Obonyo et al. 2023). Moderate AGB density estimates were found in the Southeastern region which consist of mangrove forest like Mida creek (Biswas & Biswas 2019), coastal mixed forest like Arabuko Sokoke (Mbuvi et al. 2018), and dryland forest such as Kibwezi Forest (Mwendwa Mugambi et al. 2020).

Low AGB estimates were found in the Northern and Northeastern part of Kenya which are primarily desert and semi-desert regions consisting of shrubs (Adoyo et al. 2024). In the study areas, the estimated monetary value of the carbon stored was US$ 123 million for KNFR and for US$ 3.2 million for KFR, which further underscored the effect forest ecosystem type and management practices on carbon storage potential (Cheng et al. 2024).

At low AGB values, the GEDI-RF model provided close estimates to field-measured estimates. Lahssini et al. (2024) also had similar results, highlighting the effectiveness and higher accuracy of AGB estimates from machine-learning models integrated with GEDI compared to direct measurements. We find significant variation between the two models at higher values, with the GEDI-RF model overestimating values $\leq$ 100 Mg ha$^{-1}$ and underestimating $\geq$ 200 Mg ha$^{-1}$, which were more pronounced in unmanaged tropical forest (KNFR).

Zadbagher et al. (2024) similarly reported high variation of AGB at higher values in tropical peat forest using the RF machine-learning model. On average, the GEDI-RF model estimates were higher than the field-measured estimates, owing to factors like exclusion of individual tree height as a variable in the field-measured allometric model, field measurements restricted to DBH $\geq$ 10 cm, and substitution of species-specific and site-specific allometric equations for endemic species (Dutcă et al. 2022). Chere et al. (2023) in Ethiopia, across similar ecosystem types, also used the RF model with Sentinel-1 and Sentinel-2 to achieve high accuracy of AGB using height and canopy cover predictions.

The RF machine-learning model provided a more consistent estimation of AGB compared to using GEDI alone. Further, its stable variance also suggested its reliability as a tool for predicting AGB across different forest ecosystems and improvements by integrating more predictors to refine the model under complex stands like in KNFR.

## Conclusion

Our findings highlight the effect of using integrated remote sensing approaches like the GEDI-RF model relative to field-measured model across distinct forest ecosystems in terms of forest age, stand structure dynamics and management practices.

AGB estimates from the GEDI-RF model compared to the field-measured model showed high variability with low precision in unmanaged, old-growth tropical rainforests like KNFR, and low variability with high precision in managed, urban forest ecosystems like KFR.

The integrated GEDI-RF model improved the AGB estimation accuracy by filling gaps within gridded areas where GEDI footprint was absent and provided continuous wall-to-wall spatial coverage. On average, the GEDI-RF model estimates were closer to the field measurements.

This study quantified the limitations of the GEDI-RF model relative to field-based estimates where NFI data is lacking or outdated, offering a replicable and cost-effective approach to carbon stock estimation in tropical forests monitoring. It also serves as a benchmark to support national forest policies in tropical countries that are at various stages of implementing forest carbon monitoring programs under REDD+ compliance mechanism.

Future research should explore the integration of more predictors in the RF machine-learning model to enhance the AGB estimation accuracy under different forest stand structures at large scale.

## Disclosure statement /competing interest

The author(s) declare that they have no known competing financial interests.

## Acknowledgements

We acknowledge the support of the Kenya Forestry Research Institute (KEFRI) through the collaboration agreement REF: KEFRI/56/04/VOL.1(111) with Transilvania University of Brasov, and the Friends of Karura Community Forest Association (FKF-CFA). This research was funded by a doctoral grant from Transilvania University of Brasov [Grant number DGRIAE-111284/IN1/1/EC/03.09.2021]. This research was approved by the Kenya National Commission for Science, Technology, and Innovation (NACOSTI) under license number NACOSTI/P/23/25591 and from Kenya Forest Service (KFS) under research license number REF: RESEA/1/KFS/VOL.VI (124).

## References

Adinugroho W. C., Krisnawati H., Imanuddin R., Siregar C. A., Weston C. J., & Volkova L. (2023). Developing biomass allometric equations for small trees in mixed-species forests of tropical rainforest ecozone. *Trees, Forests and People*, *13*, 100425. https://doi.org/10.1016/j.tfp.2023.100425.

Adoyo B., Kehbila A., Lutta A., Opiyo R. O., Onyango S. A., Mungo C., & Osano P. (2024). Land cover scenarios in four Kenyan arid and semi-arid regions by 2050. SEI Working Paper. Stockholm Environment Institute. https://doi.org/10.51414/sei2024.029.

Alados C. L., Sánchez-Granero M. A., Errea P., Castillo-García M., & Pueyo Y. (2022). Two dimensional searching paths exhibit fractal distribution that change with food availability (Normalized Difference Infrared Index, NDII). *Ecological Indicators*, *139*, 108940. https://doi.org/10.1016/j.ecolind.2022.108940.

Asrat Z., Eid T., Gobakken T., & Negash M. (2020). Aboveground tree biomass prediction options for the Dry Afromontane forests in south-central Ethiopia. *Forest Ecology and Management*, *473*, 118335. https://doi.org/10.1016/j.foreco.2020.118335.

Augusto L., & Boča A. (2022). Tree functional traits, forest biomass, and tree species diversity interact with site properties to drive forest soil carbon. *Nature Communications*, *13*(1), 1097. https://doi.org/10.1038/s41467-022-28748-0.

Baban G., & Niţă M.D. (2023). Measuring forest height from space. Opportunities and limitations observed in natural forests. *Measurement*, *211*, 112593. https://doi.org/10.1016/j.measurement.2023.112593.

Barinas G., Good S. P., & Tullos D. (2024). Continental Scale Assessment of Variation in Floodplain Roughness With Vegetation and Flow Characteristics. *Geophysical Research Letters*, *51*(1), e2023GL105588. https://doi.org/10.1029/2023GL105588.

Basak D., Bose A., Roy S., & Chowdhury I. R. (2023). Understanding the forest cover dynamics and its health status using GIS-based analytical hierarchy process: a study from Alipurduar district, West Bengal, India. *Water, Land, and Forest Susceptibility and Sustainability: Geospatial Approaches and Modeling*, 1, 475–508. https://doi.org/10.1016/B978-0-323-91880-0.00014-3.

Bischl B., Binder M., Lang M., Pielok T., Richter J., ..., & Lindauer, M. (2023). Hyperparameter optimization: Foundations, algorithms, best practices, and open challenges. *WIREs Data Mining and Knowledge Discovery*, *13*(2), e1484. https://doi.org/10.1002/widm.1484.

Biswas P. L., & Biswas S. R. (2019). Mangrove Forests: Ecology, Management, and Threats. In: Leal Filho W., Azul A., Brandli L., Özuyar P., Wall T. (eds) Life on Land. Encyclopedia of the UN Sustainable Development Goals (pp. 1–14). Springer, Cham. https://doi.org/10.1007/978-3-319-71065-5_26-1.

Bleher B., Uster D., & Bergsdorf T. (2006). Assessment of threat status and management effectiveness in Kakamega Forest, Kenya. *Biodiversity and Conservation*, *15*(4), 1159–1177. https://doi.org/10.1007/s10531-004-3509-3.

Boali A., Asgari H. R., Mohammadian Behbahani A., Salmanmahiny A., & Naimi B. (2024). Remotely sensed desertification modeling using ensemble of machine learning algorithms. *Remote Sensing Applications: Society and Environment*, *34*, 101149. https://doi.org/10.1016/j.rsase.2024.101149.

Borz S. A., Toaza J. M. M., & Proto A. R. (2024). Accuracy of two LiDAR-based augmented reality apps in breast height diameter measurement. *Ecological Informatics*, *81*, 102550. https://doi.org/10.1016/j.ecoinf.2024.102550

Breiman L. (2001). Random Forests. Machine Learning. *Machine Learning*, *45*(1), 5–32. https://doi.org/10.1023/A:1010933404324.

Brodie J. F., Mohd-Azlan J., Chen C., Wearn O. R., Deith M. C. M., Ball J. G. C., … Luskin M. S. (2023). Landscape-scale benefits of protected areas for tropical biodiversity. *Nature*, *620*(7975), 807–812. https://doi.org/10.1038/s41586-023-06410-z.

Bruening J., May P., Armston J., & Dubayah R. (2023). Precise and unbiased biomass estimation from GEDI data and the US Forest Inventory. *Frontiers in Forests and Global Change*, *6*. https://doi.org/10.3389/ffgc.2023.1149153.

Calders K., Brede B., Newnham G., Culvenor D., Armston J., Bartholomeus H., … & Herold M. (2023). StrucNet: a global network for automated vegetation structure monitoring. *Remote Sensing in Ecology and Conservation*, *9*(5), 587–598. https://doi.org/10.1002/rse2.333.

Cha G.-W., Moon H.-J., & Kim Y.-C. (2021). Comparison of Random Forest and Gradient Boosting Machine Models for Predicting Demolition Waste Based on Small Datasets and Categorical Variables. *International Journal of Environmental Research and Public Health*, *18*(16), 8530. https://doi.org/10.3390/ijerph18168530.

Cheng F., Tian J., He J., He H., Bao G., Yang Y., Liu G., & Zhang Z. (2024). China's future forest carbon sequestration potential under different management scenarios. *Trees, Forests and People*, *17*, 100621. https://doi.org/10.1016/j.tfp.2024.100621.

Chere Z., Zewdie W., & Biru D. (2023). Machine learning for modeling forest canopy height and cover from multi-sensor data in Northwestern Ethiopia. *Environmental Monitoring and Assessment*, *195*(12), 1452. https://doi.org/10.1007/s10661-023-12066-z.

Chirici G., Chiesi M., Fibbi L., Giannetti F., Corona P., & Maselli F. (2022). High spatial resolution modelling of net forest carbon fluxes based on ground and remote sensing data. *Agricultural and Forest Meteorology*, *316*, 108866. https://doi.org/10.1016/j.agrformet.2022.108866.

Clarke L., Wei Y.-M. (eds.) (2023). Energy Systems. In ICPP 2022: Shukla P.R. et al. (Ed.), *Climate Change 2022: Mitigation of Climate Change* (pp. 613–746). Cambridge University Press. https://doi.org/10.1017/9781009157926.008.

Cushman, K. C., Armston, J., Dubayah, R., Duncanson, L., Hancock, S., Janík, D., … & Kellner, J. R. (2023). Impact of leaf phenology on estimates of aboveground biomass density in a deciduous broadleaf forest from simulated GEDI lidar. *Environmental Research Letters*, *18*(6), 065009. https://doi.org/10.1088/1748-9326/acd2ec.

Daba, D. E., & Soromessa, T. (2019a). The accuracy of species-specific allometric equations for estimating aboveground biomass in tropical moist montane forests: Case study of *Albizia grandibracteata* and *Trichilia dregeana*. *Carbon Balance and Management*, *14*(1), 1–13. https://doi.org/10.1186/s13021-019-0134-8.

Das K. R., & Imon A. H. M. R. (2016). A Brief Review of Tests for Normality. *American Journal of Theoretical and Applied Statistics*, *5*(1), 5. https://doi.org/10.11648/j.ajtas.20160501.12.

Demarchi G., Subervie J., Catry T., & Tritsch I. (2023). Using publicly available remote sensing products to evaluate REDD <math altimg="si3.svg"> <mrow> <mo>+</mo> </mrow> </math> projects in Brazil. *Global Environmental Change*, *80*, 102653. https://doi.org/10.1016/j.gloenvcha.2023.102653.

Divasón J., Pernia-Espinoza A., & Martinez-de-Pison F. J. (2023). HYB-PARSIMONY: A hybrid approach combining Particle Swarm Optimization and Genetic Algorithms to find parsimonious models in high-dimensional datasets. *Neurocomputing*, *560*, 126840. https://doi.org/10.1016/j.neucom.2023.126840.

Dorado-Roda I., Pascual A., Godinho S., Silva C., Botequim B., Rodríguez-Gonzálvez P., González-Ferreiro E., & Guerra-Hernández J. (2021). Assessing the Accuracy of GEDI Data for Canopy Height and Aboveground Biomass Estimates in Mediterranean Forests. *Remote Sensing*, *13*(12), 2279. https://doi.org/10.3390/rs13122279.

Dubayah R., Blair J. B., Goetz S., Fatoyinbo L., Hansen M., Healey S., Hofton M., Hurtt G., Kellner J., …, & Silva, C. (2020). The Global Ecosystem Dynamics Investigation: High-resolution laser ranging of the Earth's forests and topography. *Science of Remote Sensing*, *1*, 100002. https://doi.org/10.1016/j.srs.2020.100002.

Dubayah R., Tang H., Armston J., Luthcke S., Hofton M., & Blair J. (2021). GEDI L2B Canopy Cover and Vertical Profile Metrics Data Global Footprint Level V002 [Data set]. NASA EOSDIS Land Processes Distributed Active Archive Center. https://doi.org/10.5067/GEDI/GEDI02_B.002.

Dutca I., McRoberts R. E., Næsset E., & Blujdea V. N. B. (2019). A practical measure for determining if diameter (D) and height (H) should be combined into D2H in allometric biomass models. *Forestry*, *92*(5), 627–634. https://doi.org/10.1093/forestry/cpz041.

Dutcă I., McRoberts R. E., Næsset E., & Blujdea V. N. B. (2022). Accommodating heteroscedasticity in allometric biomass models. *Forest Ecology and Management*, *505*, 119865. https://doi.org/10.1016/j.foreco.2021.119865.

Ekoungoulou R., Liu X., Loumeto J. J., & Ifo S. A. (2014). Tree Above-And Below-Ground Biomass Allometries for Carbon Stocks Estimation in Secondary Forest of Congo. *IOSR Journal of Environmental Science, Toxicology and Food Technology*, *8*(4), 09–20. https://doi.org/10.9790/2402-08420920.

EU Directorate-General for Climate Action (2024, February). International carbon pricing and markets diplomacy. The Call to Action for Paris-Aligned Carbon Markets. https://climate.ec.europa.eu/eu-action/eu-emissions-trading-system-eu-ets/international-carbon-pricing-and-markets-diplomacy_en.

Fadl M. E., AbdelRahman M. A. E., El-Desoky A. I., & Sayed Y. A. (2024). Assessing soil productivity potential in arid region using remote sensing vegetation indices. *Journal of Arid Environments*, *222*, 105166. https://doi.org/10.1016/J.JARIDENV.2024.105166.

Fagua J. C., Jantz P., Burns P., Massey R., Buitrago J. Y., Saatchi S., Hakkenberg C., & Goetz S. J. (2021). Mapping tree diversity in the tropical forest region of Chocó-Colombia. *Environmental Research Letters*, *16*(5), 054024. https://doi.org/10.1088/1748-9326/abf58a.

Fassnacht F. E., White J. C., Wulder M. A., & Næsset E. (2024). Remote sensing in forestry: current challenges, considerations and directions. *Forestry: An International Journal of Forest Research*, *97*(1), 11–37. https://doi.org/10.1093/forestry/cpad024.

Fayad I., Baghdadi N., & Lahssini K. (2022). An Assessment of the GEDI Lasers' Capabilities in Detecting Canopy Tops and Their Penetration in a Densely Vegetated, Tropical Area. *Remote Sensing*, *14*(13), 2969. https://doi.org/10.3390/rs14132969.

Feitosa T. B., Fernandes M. M., Santos C. A. G., Silva R. M. da, Garcia J. R., ... & Cunha, E. R. da. (2023). Assessing economic and ecological impacts of carbon stock and land use changes in Brazil's Amazon Forest: A 2050

projection. *Sustainable Production and Consumption*, *41*, 64–74. https://doi.org/10.1016/j.spc.2023.07.009.

Feukeng S. S. K., Maffo L. N., Nguetsop V. F., Rossi V., Chimi C. D., Wouokoue B. J. T., & Kengne C. O. (2020). Single-species allometric equations for above-ground biomass of most abundant long-lived pioneer species in semi-deciduous rain forests of the central region of Cameroon. *World Journal of Advanced Research and Reviews*, *7*(2), 336–348. https://doi.org/10.30574/wjarr.2020.7.2.0288.

Ferreira M. P., Martins G. B., de Almeida T. M. H., da Silva Ribeiro R., da Veiga Júnior V. F., … & Kurtz B. C. (2024). Estimating aboveground biomass of tropical urban forests with UAV-borne hyperspectral and LiDAR data. *Urban Forestry & Urban Greening*, *96*, 128362. https://doi.org/10.1016/j.ufug.2024.128362.

Francini S., Cavalli A., D'Amico G., McRoberts R. E., Maesano M., Munafò M., Scarascia Mugnozza G., & Chirici G. (2023). Reusing Remote Sensing-Based Validation Data: Comparing Direct and Indirect Approaches for Afforestation Monitoring. *Remote Sensing*, *15*(6), 1638. https://doi.org/10.3390/rs15061638.

Gelabert P. J., Rodrigues M., Coll L., Vega-Garcia C., & Ameztegui A. (2024). Maximum tree height in European Mountains decreases above a climate-related elevation threshold. *Communications Earth & Environment*, *5*(1), 84. https://doi.org/10.1038/s43247-024-01246-5.

Giavarina D. (2015). Understanding Bland Altman analysis. *Biochemia Medica*, *25*(2), 141–151. https://doi.org/10.11613/BM.2015.015.

Gonçalves F., Treuhaft R., Law B., Almeida A., Walker W., Baccini A., Dos Santos J., & Graça P. (2017). Estimating Aboveground Biomass in Tropical Forests: Field Methods and Error Analysis for the Calibration of Remote Sensing Observations. *Remote Sensing*, *9*(1), 47. https://doi.org/10.3390/rs9010047.

Hakkenberg C. R., Tang H., Burns P., & Goetz S. J. (2023). Canopy structure from space using <scp>GEDI</scp> lidar. *Frontiers in Ecology and the Environment*, *21*(1), 55–56. https://doi.org/10.1002/fee.2585.

Hancock S., Armston J., Hofton M., Sun X., Tang H., Duncanson L. I., Kellner J. R., & Dubayah R. (2019a). The GEDI Simulator: A Large-Footprint Waveform Lidar Simulator for Calibration and Validation of Spaceborne Missions. *Earth and Space Science*, *6*(2), 294–310. https://doi.org/10.1029/2018EA000506.

Hancock S., Armston J., Hofton M., Sun X., Tang H., Duncanson L. I., Kellner J. R., & Dubayah R. (2019b). The GEDI Simulator: A Large-Footprint Waveform Lidar Simulator for Calibration and Validation of Spaceborne Missions. *Earth and Space Science*, *6*(2), 294–310. https://doi.org/10.1029/2018EA000506.

Hansen M. C., Potapov P. V., Moore R., Hancher M., Turubanova S. A., Tyukavina A., Thau D., … & Townshend J. R. G. (2013). High-Resolution Global Maps of 21st-Century Forest Cover Change. *Science*, *342*(6160), 850–853. https://doi.org/10.1126/science.1244693.

Hemingway H., & Opalach D. (2024). Integrating Lidar Canopy Height Models with Satellite-Assisted Inventory Methods: A Comparison of Inventory Estimates. *Forest Science*, *70*(1), 2–13. https://doi.org/10.1093/forsci/fxad047.

Hunka N., Duncanson L., Armston J., Dubayah R., Healey S. P., Santoro M., May P., Araza A., … Melo J. (2024). Intergovernmental Panel on Climate Change (IPCC) Tier 1 forest biomass estimates from Earth Observation. *Scientific Data*, *11*(1), 1127. https://doi.org/10.1038/s41597-024-03930-9.

Jia D., Wang C., Hakkenberg C. R., Numata I., Elmore A. J., & Cochrane M. A. (2024). Accuracy evaluation and effect factor analysis of GEDI aboveground biomass product for temperate forests in the conterminous United States. *GIScience & Remote Sensing*, *61*(1). https://doi.org/10.1080/15481603.2023.2292374.

Joshi N., Mitchard E. T. A., Brolly M., Schumacher J., Fernández-Landa A., Johannsen V. K., Marchamalo M., & Fensholt R. (2017). Understanding 'saturation' of radar signals over forests. *Scientific Reports*, *7*(1), 3505. https://doi.org/10.1038/s41598-017-03469-3.

Keige E. W. (2019). Impact of Benefit Sharing Arrangements on Sustainable Management of Public Forests: a Case Study of Karura Forest in Kenya. PhD Thesis. University of Nairobi.

Kellner J. R., Armston J., & Duncanson L. (2023). Algorithm Theoretical Basis Document for GEDI Footprint Aboveground Biomass Density. *Earth and Space Science*, *10*(4). https://doi.org/10.1029/2022EA002516.

Khajavi H., & Rastgoo A. (2023). Predicting the carbon dioxide emission caused by road transport using a Random Forest (RF) model combined by Meta-Heuristic Algorithms. *Sustainable Cities and Society*, *93*, 104503. https://doi.org/10.1016/j.scs.2023.104503

Kikuchi Y., Ouchida K., Kanematsu Y., & Okubo T. (2018). Design Support of Smart Energy Systems based on Locally Available Resources: A Case Study in Isolated Islands in Japan (pp. 2515–2520). https://doi.org/10.1016/B978-0-444-64241-7.50414-6.

Kipkorir T. G. (2017). Modelling impacts of climate change on tree biomass and distribution in Arabuko Sokoke forest reserve, Kenya. University of Nairobi.

Krause P., Forbes B., Barajas-Ritchie A., Clark M., Disney M., Wilkes P., & Bentley L. P. (2023). Using terrestrial laser scanning to evaluate non-destructive aboveground biomass allometries in diverse Northern California forests. *Frontiers in Remote Sensing*, *4*. https://doi.org/10.3389/frsen.2023.1132208.

Krzywinski M., & Altman N. (2014). Comparing samples—part I. *Nature Methods*, *11*(3), 215–216. https://doi.org/10.1038/nmeth.2858.

Kuyah S., Dietz J., Muthuri C., Jamnadass R., Mwangi P., Coe R., & Neufeldt H. (2012). Allometric equations for estimating biomass in agricultural landscapes: I. Aboveground biomass. *Agriculture, Ecosystems & Environment*, *158*, 216–224. https://doi.org/10.1016/j.agee.2012.05.011.

Lahssini K., Baghdadi N., Le Maire G., Dupuy S., & Fayad I. (2024). Use of GEDI Signal and Environmental

Parameters to Improve Canopy Height Estimation over Tropical Forest Ecosystems in Mayotte Island. *Canadian Journal of Remote Sensing*, *50*(1). https://doi.org/10.1080/07038992.2024.2351004.

Lee J., Kim J., Hahn S., Han H., Shin G., Kim W.-C., & Yoon S.-W. (2024). Data-driven disruption prediction using random forest in KSTAR. *Fusion Engineering and Design*, *199*, 114128. https://doi.org/10.1016/j.fusengdes.2023.114128.

Lei Q., Yu H., & Lin Z. (2024). Understanding China's CO2 emission drivers: Insights from random forest analysis and remote sensing data. *Heliyon*, *10*(7), e29086. https://doi.org/10.1016/j.heliyon.2024.e29086.

Li H., Li X., Kato T., Hayashi M., Fu J., & Hiroshima T. (2024). Accuracy assessment of GEDI terrain elevation, canopy height, and aboveground biomass density estimates in Japanese artificial forests. *Science of Remote Sensing*, *10*, 100144. https://doi.org/10.1016/j.srs.2024.100144.

Lindberg L. (2020). Forest data acquisition with the application Arboreal Forest – A study about measurement precision, accuracy and efficiency. Umeå: SLU, Department of Forest Biomaterials and Technology. https://stud.epsilon.slu.se/15456/.

Lisboa S. N., Guedes B. S., Ribeiro N., & Sitoe A. (2018). Biomass allometric equation and expansion factor for a mountain moist evergreen forest in Mozambique. *Carbon Balance and Management*, *13*(1), 23. https://doi.org/10.1186/s13021-018-0111-7.

Liu A., Chen Y., & Cheng X. (2024). Evaluating ICESat-2 and GEDI with Integrated Landsat-8 and PALSAR-2 for Mapping Tropical Forest Canopy Height. *Remote Sensing*, *16*(20), 3798. https://doi.org/10.3390/rs16203798.

Ma T., Zhang C., Ji L., Zuo Z., Beckline M., Hu Y., Li X., & Xiao X. (2024). Development of forest aboveground biomass estimation, its problems and future solutions: A review. *Ecological Indicators*, *159*, 111653. https://doi.org/10.1016/j.ecolind.2024.111653.

Magruder L. A., Farrell S. L., Neuenschwander A., Duncanson L., Csatho B., Kacimi S., & Fricker H. A. (2024). Monitoring Earth's climate variables with satellite laser altimetry. *Nature Reviews Earth & Environment*, *5*(2), 120–136. https://doi.org/10.1038/s43017-023-00508-8.

Malimbwi R. E., & Chamshama S. (2016). *Allometric volume and biomass models in Tanzania*. https://doi.org/10.13140/RG.2.1.1891.5445.

Manji A. (2017). Property, conservation, and enclosure in Karura Forest, Nairobi. *African Affairs*, *116*(463), 186–205. https://doi.org/10.1093/afraf/adx006.

Mbuvi M. T. E., Ndalilo L., & Hussein A. (2018). Applying Sustainability and Ethics in Forest Management and Community Livelihoods: A Case Study from Arabuko Sokoke Forest, Kenya. *Open Journal of Forestry*, *08*(04), 532–552. https://doi.org/10.4236/ojf.2018.84033.

Mellor A., Boukir S., Haywood A., & Jones S. (2015). Exploring issues of training data imbalance and mislabelling on random forest performance for large area land cover classification using the ensemble margin. *ISPRS Journal of Photogrammetry and Remote Sensing*, *105*, 155–168. https://doi.org/10.1016/j.isprsjprs.2015.03.014.

Mohite J., Sawant S., Pandit A., Sakkan M., Pappula S., & Parmar A. (2024). Forest aboveground biomass estimation by GEDI and multi-source EO data fusion over Indian forest. *International Journal of Remote Sensing*, *45*(4), 1304–1338. https://doi.org/10.1080/01431161.2024.2307944.

Morgan E. A., Bush G., Mandea J. Z., & Maraseni T. (2023). Community evaluation of forest and REDD+ governance quality in the Democratic Republic of the Congo. *Journal of Environmental Management*, *328*, 116891. https://doi.org/10.1016/j.jenvman.2022.116891.

Moundounga Mavouroulou Q., Ngomanda A., Engone Obiang N. L., Lebamba J., Gomat H., … & Picard N. (2014). How to improve allometric equations to estimate forest biomass stocks? Some hints from a central African forest. *Canadian Journal of Forest Research*, *44*(7), 685–691. https://doi.org/10.1139/cjfr-2013-0520.

Mulatu A., Negash M., & Asrat Z. (2024). Species-specific allometric models for reducing uncertainty in estimating above ground biomass at Moist Evergreen Afromontane Forest of Ethiopia. *Scientific Reports*, *14*(1), 1147. https://doi.org/10.1038/s41598-023-51002-6.

Munteanu C., Kraemer B. M., Hansen H. H., Miguel S., Milner-Gulland E. J., ... & Kuemmerle T. (2024). The potential of historical spy-satellite imagery to support research in ecology and conservation. *BioScience*. https://doi.org/10.1093/biosci/biae002.

Murrins Misiukas J., Carter S., & Herold M. (2021). Tropical Forest Monitoring: Challenges and Recent Progress in Research. *Remote Sensing*, *13*(12), 2252. https://doi.org/10.3390/rs13122252.

Mwendwa Mugambi, J., Kagendo J., Kweyu M., & Mbuvi M. T. E. (2020). Influence of Community Forest Association Activities on Dryland Resources Management: Case of Kibwezi Forest in Kenya. *International Journal of Natural Resource Ecology and Management*, *5*(3), 119. https://doi.org/10.11648/j.ijnrem.20200503.16.

Nandy S., Srinet R., & Padalia H. (2021). Mapping Forest Height and Aboveground Biomass by Integrating ICESat-2, Sentinel-1 and Sentinel-2 Data Using Random Forest Algorithm in Northwest Himalayan Foothills of India. *Geophysical Research Letters*, *48*(14). https://doi.org/10.1029/2021GL093799.

Narin O. G., Abdikan S., Gullu M., Lindenbergh R., Balik Sanli F., & Yilmaz I. (2024). Improving global digital elevation models using space-borne GEDI and ICESat-2 LiDAR altimetry data. *International Journal of Digital Earth*, *17*(1). https://doi.org/10.1080/17538947.2024.2316113.

NASA Jet Propulsion Laboratory (2024). *NASA Jet Propulsion Laboratory (JPL) - Robotic Space Exploration*. https://www.jpl.nasa.gov/.

Navarro J. A., Algeet N., Fernández-Landa A., Esteban J., Rodríguez-Noriega P., & Guillén-Climent M. L. (2019). Integration of UAV, Sentinel-1, and Sentinel-2 Data for Mangrove Plantation Aboveground Biomass Monitoring in Senegal. *Remote Sensing*, *11*(1), 77. https://doi.org/10.3390/rs11010077.

Nesha K., Herold M., De Sy V., Duchelle A. E., Martius C., Branthomme A., Garzuglia M., Jonsson O., &

Pekkarinen A. (2021). An assessment of data sources, data quality and changes in national forest monitoring capacities in the Global Forest Resources Assessment 2005–2020. *Environmental Research Letters*, *16*(5), 054029. https://doi.org/10.1088/1748-9326/abd81b.

Nieto P. J. G., Gonzalo E. G., García L. A. M., Prado L. Á., & Sánchez A. B. (2024). Predicting the critical superconducting temperature using the random forest, MLP neural network, M5 model tree and multivariate linear regression. *Alexandria Engineering Journal*, *86*, 144–156. https://doi.org/10.1016/j.aej.2023.11.034.

Niu W., Ha Y., & Chi N. (2020). Support vector machine based machine learning method for GS 8QAM constellation classification in seamless integrated fiber and visible light communication system. *Science China Information Sciences*, *63*(10), 202306. https://doi.org/10.1007/s11432-019-2850-3.

Nyamukuru A., Whitney C., Tabuti, J. R. S., Esaete J., & Low M. (2023). Allometric models for aboveground biomass estimation of small trees and shrubs in African savanna ecosystems. *Trees, Forests and People*, *11*, 100377. https://doi.org/10.1016/j.tfp.2023.100377.

Obonyo O. A., Agevi H., & Tsingalia M. H. (2023). Aboveground carbon stocks and its functional relationship with tree species diversity: the case of Kakamega and North Nandi Forests, Kenya. *Scientific Reports*, *13*(1), 20921. https://doi.org/10.1038/s41598-023-47871-6.

Osewe E. O., & Dutcă I. (2021). The Effects of Combining the Variables in Allometric Biomass Models on Biomass Estimates over Large Forest Areas: A European Beech Case Study. *Forests*, *12*(10), 1428. https://doi.org/10.3390/f12101428.

Osewe E. O., Niţă M. D., & Abrudan I. V. (2022). Assessing the Fragmentation, Canopy Loss and Spatial Distribution of Forest Cover in Kakamega National Forest Reserve, Western Kenya. *Forests*, *13*(12). https://doi.org/10.3390/f13122127.

Pascual A., Guerra-Hernández J., Armston J., Minor D. M., Duncanson L. I., May P. B., Kellner J. R., & Dubayah R. (2023). Assessing the performance of NASA's GEDI L4A footprint aboveground biomass density models using National Forest Inventory and airborne laser scanning data in Mediterranean forest ecosystems. *Forest Ecology and Management*, *538*, 120975. https://doi.org/10.1016/j.foreco.2023.120975.

Pascual A., May P. B., Cárdenas-Martínez A., Guerra-Hernández J., Hunka N., …. & Dubayah R. O. (2025). Calibration of GEDI footprint aboveground biomass models in Mediterranean forests with NFI plots: A comparison of approaches. *Journal of Environmental Management*, *375*, 124313. https://doi.org/10.1016/j.jenvman.2025.124313.

Pati P. K., Kaushik P., Khan M. L., & Khare P. K. (2022). Allometric equations for biomass and carbon stock estimation of small diameter woody species from tropical dry deciduous forests: Support to REDD+. *Trees, Forests and People*, *9*, 100289. https://doi.org/10.1016/j.tfp.2022.100289.

Picard N., Saint-André L., & Henry M. (2012). Manual for building tree volume and biomass allometric equations: from field measurement to prediction. FAO & CIRAD.

Potapov P., Li X., Hernandez-Serna A., Tyukavina A., Hansen M. C., Kommareddy A., ... & Hofton M. (2021). Mapping global forest canopy height through integration of GEDI and Landsat data. *Remote Sensing of Environment*, *253*, 112165. https://doi.org/10.1016/j.rse.2020.112165.

Prayogo, C., Muthahar C., & Ishaq R. M. (2021). Allometric equation of local bamboo for estimating carbon sequestration of bamboo riparian forest. *IOP Conference Series: Earth and Environmental Science*, *905*(1), 012002. https://doi.org/10.1088/1755-1315/905/1/012002.

Pretzsch H., Rötzer T., & Forrester D. I. (2017). Modelling Mixed-Species Forest Stands. In *Mixed-Species Forests* (pp. 383–431). Springer Berlin Heidelberg. https://doi.org/10.1007/978-3-662-54553-9_8.

Probst P., Wright M. N., & Boulesteix A. (2019). Hyperparameters and tuning strategies for random forest. *WIREs Data Mining and Knowledge Discovery*, *9*(3). https://doi.org/10.1002/widm.1301.

QGIS Project (2023). *Gentle GIS Introduction QGIS Project*. https://docs.qgis.org/3.34/en/docs/index.html.

Quiros E., Polo, M.-E., & Fragoso-Campon, L. (2021). GEDI Elevation Accuracy Assessment: A Case Study of Southwest Spain. *IEEE Journal of Selected Topics in Applied Earth Observations and Remote Sensing*, *14*, 5285–5299. https://doi.org/10.1109/JSTARS.2021.3080711.

Ramachandran N., Saatchi S., Tebaldini S., d'Alessandro M. M., & Dikshit O. (2023). Mapping tropical forest aboveground biomass using airborne SAR tomography. *Scientific Reports*, *13*(1), 6233. https://doi.org/10.1038/s41598-023-33311-y.

Ramampiandra E. C., Scheidegger A., Wydler J., & Schuwirth N. (2023). A comparison of machine learning and statistical species distribution models: Quantifying overfitting supports model interpretation. *Ecological Modelling*, *481*, 110353. https://doi.org/10.1016/j.ecolmodel.2023.110353.

Republic of Kenya (2016). Forest Conservation and Management Act. *Forest Conservation and Management Act*, *155*(34), 677–736. http://www.ilo.org/dyn/travail/docs/505/Employment Act 2007.pdf.

Rey D., & Neuhäuser M. (2011). Wilcoxon-Signed-Rank Test. In *International Encyclopedia of Statistical Science* (pp. 1658–1659). Springer Berlin Heidelberg. https://doi.org/10.1007/978-3-642-04898-2_616.

Rodrigues de Moura Fernandes M., Fernandes da Silva G., Quintão de Almeida A., Marques Fernandes M., Ribeiro de Mendonça A., ... & Pereira Martins Silva J. (2023). Aboveground biomass estimation in dry forest in northeastern Brazil using metrics extracted from sentinel-2 data: Comparing parametric and non-parametric estimation methods. *Advances in Space Research*, *72*(2), 361–377. https://doi.org/10.1016/j.asr.2023.03.010.

Rojas-García F., De Jong B. H. J., Martínez-Zurimendí P., & Paz-Pellat F. (2015). Database of 478 allometric equations to estimate biomass for Mexican trees and

forests. *Annals of Forest Science*, *72*(6), 835–864. https://doi.org/10.1007/s13595-015-0456-y.

Rozendaal D. M. A., Requena Suarez D., De Sy V., Avitabile V., Carter S., Adou Yao C. Y., … Herold M. (2022). Aboveground forest biomass varies across continents, ecological zones and successional stages: refined IPCC default values for tropical and subtropical forests. *Environmental Research Letters*, *17*(1), 014047. https://doi.org/10.1088/1748-9326/ac45b3.

Sandim A., Amaro M., Silva M. E., Cunha J., Morais S., Marques A., Ferreira A., Lousada J. L., & Fonseca T. (2023). New Technologies for Expedited Forest Inventory Using Smartphone Applications. *Forests*, *14*(8), 1553. https://doi.org/10.3390/f14081553.

Sarkar D. P., Uma Shankar B., & Ranjan Parida B. (2024). A novel approach for retrieving GPP of evergreen forest regions of India using random forest regression. *Remote Sensing Applications: Society and Environment*, *33*, 101116. https://doi.org/10.1016/j.rsase.2023.101116.

Schneider A., Blick T., Pauls S. U., & Dorow W. H. O. (2021). The list of forest affinities for animals in Central Europe – A valuable resource for ecological analysis and monitoring in forest animal communities? *Forest Ecology and Management*, *479*, 118542. https://doi.org/10.1016/j.foreco.2020.118542.

Sebrala H., Abich A., Negash M., Asrat Z., & Lojka B. (2022a). Tree allometric equations for estimating biomass and volume of Ethiopian forests and establishing a database: Review. *Trees, Forests and People*, *9*, 100314. https://doi.org/10.1016/j.tfp.2022.100314.

Sebrala H., Abich A., Negash M., Asrat Z., & Lojka B. (2022b). Tree allometric equations for estimating biomass and volume of Ethiopian forests and establishing a database: Review. *Trees, Forests and People*, *9*, 100314. https://doi.org/10.1016/j.tfp.2022.100314.

Shannon E. S., Finley A. O., Hayes D. J., Noralez S. N., Weiskittel A. R., Cook B. D., & Babcock C. (2022). *Quantifying and correcting geolocation error in sampling LiDAR forest canopy observations using high spatial accuracy ALS: A case study involving GEDI*. https://doi.org/10.1002/env.2840.

Shi Y., Gao J., Li X., Li J., dela Torre D. M. G., & Brierley G. J. (2021). Improved Estimation of Aboveground Biomass of Disturbed Grassland through Including Bare Ground and Grazing Intensity. *Remote Sensing*, *13*(11), 2105. https://doi.org/10.3390/rs13112105.

Silva C. A., Duncanson L., Hancock S., Neuenschwander A., Thomas N., Hofton M., ..., & Dubayah R. (2021). Fusing simulated GEDI, ICESat-2 and NISAR data for regional aboveground biomass mapping. *Remote Sensing of Environment*, *253*, 112234. https://doi.org/10.1016/j.rse.2020.112234.

Silva C. A., Saatchi S., Garcia M., Labriere N., Klauberg C., Ferraz A., … & Hudak A. T. (2018). Comparison of Small- and Large-Footprint Lidar Characterization of Tropical Forest Aboveground Structure and Biomass: A Case Study from Central Gabon. *IEEE Journal of Selected Topics in Applied Earth Observations and Remote Sensing*, *11*(10), 3512–3526. https://doi.org/10.1109/JSTARS.2018.2816962.

Singha C., & Sahoo S. (2024). Predicting Forest Canopy Height Using GEDI LiDAR Based Machine Learning Technique Over Similipal Biosphere, India. In: Pradhan B., Mukhopadhyay S. (eds) IoT Sensors, ML, AI and XAI: Empowering A Smarter World. Smart Sensors, Measurement and Instrumentation (vol. 50, pp. 363–374). Springer, Cham. https://doi.org/10.1007/978-3-031-68602-3_18.

Stan K. D., Sanchez-Azofeifa, A., & Hamann, H. F. (2024). Widespread degradation and limited protection of forests in global tropical dry ecosystems. *Biological Conservation*, *289*, 110425. https://doi.org/10.1016/j.biocon.2023.110425.

Sun Z., Wang, G., Li, P., Wang, H., Zhang, M., & Liang, X. (2024). An improved random forest based on the classification accuracy and correlation measurement of decision trees. *Expert Systems with Applications*, *237*, 121549. https://doi.org/10.1016/j.eswa.2023.121549.

Tadese S., Soromessa T., Aneseye A. B., Gebeyehu G., Noszczyk T., & Kindu M. (2023). The impact of land cover change on the carbon stock of moist afromontane forests in the Majang Forest Biosphere Reserve. *Carbon Balance and Management*, *18*(1), 24. https://doi.org/10.1186/s13021-023-00243-z.

Tarus G. K., & Nadir S. W. (2020). Effect of Forest Management Types on Soil Carbon Stocks in Montane Forests: A Case Study of Eastern Mau Forest in Kenya. *International Journal of Forestry Research*, *2020*, 1–10. https://doi.org/10.1155/2020/8862813.

Tetere V., & Zeverte-Rivza S. (2023). Closing Data Gaps to Measure the Bioeconomy in the EU. *Biomass*, *3*(2), 108–122. https://doi.org/10.3390/biomass3020008.

Tian L., Wu X., Tao Y., Li M., Qian C., Liao L., & Fu W. (2023). Review of Remote Sensing-Based Methods for Forest Aboveground Biomass Estimation: Progress, Challenges, and Prospects. *Forests*, *14*(6), 1086. https://doi.org/10.3390/f14061086.

Tom Dieck M. C., Jung T. H., & Loureiro S. M. C. (Eds.) (2021). Augmented Reality and Virtual Reality. New Trends in Immersive Technology. Springer International Publishing. https://doi.org/10.1007/978-3-030-68086-2.

Tomppo E. (2004). Resource Assessment | Forest Resources. In *Encyclopedia of Forest Sciences* (pp. 965–973). Elsevier. https://doi.org/10.1016/B0-12-145160-7/00156-3.

Tumwebaze S. B., Bevilacqua E., Briggs R., & Volk T. (2013). Allometric biomass equations for tree species used in agroforestry systems in Uganda. *Agroforestry Systems*, *87*(4), 781–795. https://doi.org/10.1007/s10457-013-9596-y.

Ullah F., Gilani H., Sanaei A., Hussain K., & Ali A. (2021). Stand structure determines aboveground biomass across temperate forest types and species mixture along a local-scale elevational gradient. *Forest Ecology and Management*, *486*, 118984. https://doi.org/10.1016/j.foreco.2021.118984.

Urbazaev M., Hess L. L., Hancock S., Sato L. Y., Ometto J. P., .... & Schmullius C. (2022). Assessment of terrain elevation estimates from ICESat-2 and GEDI spaceborne LiDAR missions across different land cover and forest types. *Science of Remote Sensing*, *6*, 100067. https://doi.org/10.1016/j.srs.2022.100067.

Vrtač T., Ocepek D., Česnik M., Čepon G., & Boltežar M. (2024). A hybrid modeling strategy for training data generation in machine learning-based structural health monitoring. *Mechanical Systems and Signal Processing*, *207*, 110937. https://doi.org/10.1016/j.ymssp.2023.110937.

Vuillod B., Zani M., Hallo L., & Montemurro M. (2024). Handling noise and overfitting in surrogate models based on non-uniform rational basis spline entities. *Computer Methods in Applied Mechanics and Engineering*, *425*, 116913. https://doi.org/10.1016/j.cma.2024.116913.

Wang C., Zhang W., Ji Y., Marino A., Li C., Wang L., Zhao H., & Wang M. (2024a). Correction: Wang et al. Estimation of Aboveground Biomass for Different Forest Types Using Data from Sentinel-1, Sentinel-2, ALOS PALSAR-2, and GEDI. Forests 2024, 15, 215. *Forests*, *15*(3), 401. https://doi.org/10.3390/f15030401.

Wang W., Han F., Kong Z., Ling H., & Hao X. (2024b). The maximum threshold of vegetation restoration (EVI-Area) in typical watersheds of arid regions under water constraints. *Ecological Indicators*, *158*, 111580. https://doi.org/10.1016/j.ecolind.2024.111580.

Wen D., Zhu S., Tian Y., Guan X., & Lu Y. (2024). Generating 10-Meter Resolution Land Use and Land Cover Products Using Historical Landsat Archive Based on Super Resolution Guided Semantic Segmentation Network. *Remote Sensing*, *16*(12), 2248. https://doi.org/10.3390/rs16122248.

Yao Z., Xin Y., Yang L., Zhao L., & Ali A. (2022). Precipitation and temperature regulate species diversity, plant coverage and aboveground biomass through opposing mechanisms in large-scale grasslands. *Frontiers in Plant Science*, *13*. https://doi.org/10.3389/fpls.2022.999636.

Yohannes H., & Soromessa T. (2015). Carbon Stock Analysis along Slope and Slope Aspect Gradient in Gedo Forest: Implications for Climate Change Mitigation. *Journal of Earth Science & Climatic Change*, *06*(09). https://doi.org/10.4172/2157-7617.1000305.

Zadbagher E., Marangoz A., & Becek K. (2024). Estimation of above-ground biomass using machine learning approaches with InSAR and LiDAR data in tropical peat swamp forest of Brunei Darussalam. *IForest - Biogeosciences and Forestry*, *17*(3), 172–179. https://doi.org/10.3832/ifor4434-017.

Zhang S., Vega C., Deleuze C., Durrieu S., Barbillon P., Bouriaud O., & Renaud J.-P. (2022). Modelling forest volume with small area estimation of forest inventory using GEDI footprints as auxiliary information. *International Journal of Applied Earth Observation and Geoinformation*, *114*, 103072. https://doi.org/10.1016/j.jag.2022.103072.

Zhang X., Shen H., Huang T., Wu Y., Guo B., Liu Z., Luo H., Tang J., Zhou H., Wang L., Xu W., & Ou G. (2024). Improved random forest algorithms for increasing the accuracy of forest aboveground biomass estimation using Sentinel-2 imagery. *Ecological Indicators*, *159*, 111752. https://doi.org/10.1016/j.ecolind.2024.111752.

Zhao P., Lu D., Wang G., Wu C., Huang Y., & Yu S. (2016). Examining Spectral Reflectance Saturation in Landsat Imagery and Corresponding Solutions to Improve Forest Aboveground Biomass Estimation. *Remote Sensing*, *8*(6), 469. https://doi.org/10.3390/rs8060469.

Zhu X., Wang C., Nie S., Pan F., Xi X., & Hu Z. (2020). Mapping forest height using photon-counting LiDAR data and Landsat 8 OLI data: A case study in Virginia and North Carolina, USA. *Ecological Indicators*, *114*, 106287. https://doi.org/10.1016/j.ecolind.2020.106287.